

Estimation of Natural Convection Heat Transfer from Plate-Fin Heat Sinks in a Closed Enclosure

Han-Taw Chen, Chung-Hou Lai, Tzu-Hsiang Lin, Ge-Jang He

Abstract—This study applies the inverse method and three-dimensional CFD commercial software in conjunction with the experimental temperature data to investigate the heat transfer and fluid flow characteristics of the plate-fin heat sink in a closed rectangular enclosure for various values of fin height. The inverse method with the finite difference method and the experimental temperature data is applied to determine the heat transfer coefficient. The $k-\varepsilon$ turbulence model is used to obtain the heat transfer and fluid flow characteristics within the fins. To validate the accuracy of the results obtained, the comparison of the average heat transfer coefficient is made. The calculated temperature at selected measurement locations on the plate-fin is also compared with experimental data.

Keywords—Inverse method, FLUENT, $k-\varepsilon$ model, Heat transfer characteristics, Plate-fin heat sink.

I. INTRODUCTION

NATURAL convection heat transfer with heat sink and extended surfaces has been widely used in engineering applications. In recent years, with the rapid development of electronic technology, promoting the heat transfer rate under the working process at the desired operating temperature may play an important role to ensure reliable operation of the electronic components. The appropriate design of the heat sink has gradually become attractive for these applications because they provide a more economical solution to the above problem.

A great amount of research has been devoted to predict natural convection heat transfer between two plate-fins. Elenbass [1] studied the natural convection heat transfer for different values of the fin size, temperature and inclination angle. Sparrow and Bahrami [2] showed the heat transfer coefficient between the two vertical plate-fins with different fin spacing through experiments and conclusions from [1]. Bodoia and Osterle [3] applied numerical method to study the heat transfer and flow characteristic between the two vertical plate-fins.

In order to increase the heat transfer rate of the heat sink under natural convection heat transfer, numerous investigations have been conducted to study heat transfer and empirical correlation of rectangular fins. Vollaro et al. [4] found the optimum fin spacing for the plate-fins on a vertical plate. Baskaya et al. [5] applied numerical method to investigate the optimum fin spacing for the plate fins on a horizontal plate. Harahap and Setio [6] obtained empirical correlation for the plate fins on the horizontal and vertical plate by the experiment.

For many engineering applications, the heat sink was often placed in a closed enclosure. This has forced many researchers to study the natural convection heat transfer and fluid flow in closed enclosure. Nada [7] obtained empirical relationship of natural convection heat transfer in the horizontal and vertical closed narrow enclosure with the fins on a heated rectangular plate by the experiment. Yalcin et al. [8] applied the finite volume method to investigate the optimum fin spacing and fin height in limited enclosure. Tari and Mehrtash [9] applied ANSYS FLUENT solver with zero-equation turbulence model to investigate the natural convection heat transfer from the inclined plate-fin heat sinks. Their suggested correlations were in good agreement with literature data. However, it can be found from [7]-[9] that the calculated temperature did not compare with the experimental data at the selected measurement locations on the fin.

The present study further applies the inverse method and the commercial software FLUENT [10] in conjunction with the $k-\varepsilon$ turbulence model and the experimental temperature data to determine the heat transfer characteristics within the fins on a heated horizontal plate for various values of the air velocity and the fin spacing. The results also show that the number of the total grid points may slightly increase with the fin spacing. The comparison of the average heat transfer coefficient will be made in order to validate the accuracy of the results obtained. The calculated temperature at selected measurement locations on the middle fin is also compared with experimental data.

II. MATHEMATICAL FORMULATION OF INVERSE SCHEME

The two-dimensional inverse heat conduction problem is first introduced to estimate the unknown heat transfer coefficient on the fins of the plate-fin heat sinks for various values of the fin height. The temperature of the fin at the selected measurement locations and the ambient air temperature are measured from the experimental apparatus constructed in a closed rectangular enclosure. The inverse method in conjunction with the finite difference method, the experimental temperature data and least squares method is used to predict the heat transfer coefficient for the three vertical fins attached to a heated horizontal plate. Due to the assumption of non-uniform distribution of heat transfer coefficient, the entire fin is divided into several sub-fin regions before performing an inverse method.

The heat transfer coefficient in each sub-fin region is assumed to be an unknown constant. The measurement locations and sub-fin regions is shown in Fig. 1.

Han-Taw Chen is with Department of Mechanical Engineering, National Cheng Kung University, Tainan 701, Taiwan (Phone: +886-6-2757575-62157; e-mail: htchen@mail.ncku.edu.tw).

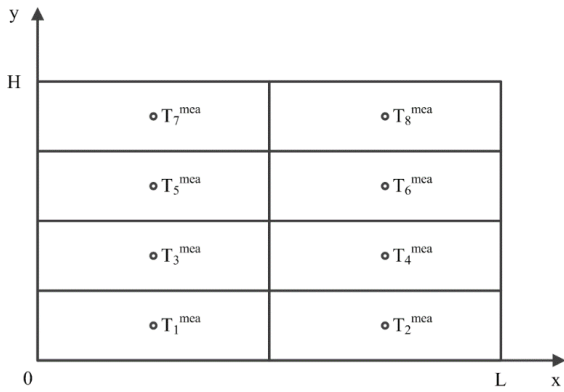


Fig. 1 Physical geometry of the measurement locations and sub-fin regions

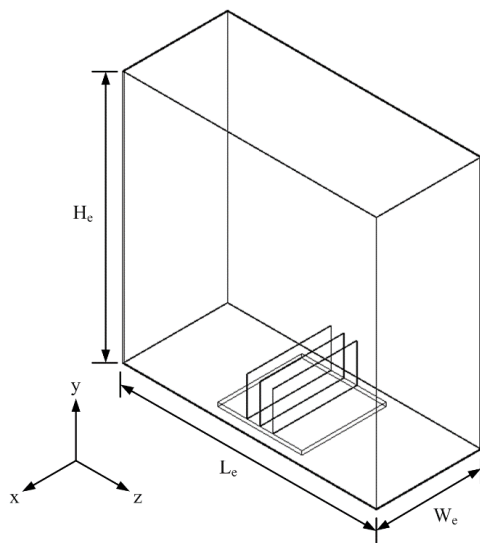


Fig. 2 Three parallel rectangular fins mounted on the top surface of a horizontal plate in a rectangular enclosure

Under the assumption of the thin fin, the temperature gradient in the z-direction (the fin thickness) can be neglected and the fin temperature varies only in the x- and y-directions. Moreover, the total surface area of the edge of the fin relative to the total surface area of the fin is small enough. This implies that the actual heat transfer rate dissipated through the fin tip is much smaller than the total heat transfer rate drawn from the fin base. Thus, the boundary conditions at the edge surface of the fins may be assumed to be insulated [11], [12]. Under the assumption of steady state and constant thermal properties, the heat conduction equation for a thin fin can be expressed as

$$\frac{\partial^2 T}{\partial x^2} + \frac{\partial^2 T}{\partial y^2} = \frac{2h(x,y)}{k_f t} (T - T_\infty), \quad 0 < x < L, 0 < y < H \quad (1)$$

Its corresponding boundary conditions are

$$\frac{\partial T}{\partial x} = 0 \quad \text{at } x = 0 \text{ and } x = L \quad (2)$$

$$T(x, 0) = T_0 \quad \text{at } y = 0 \quad (3)$$

and

$$\frac{\partial T}{\partial y} = 0 \quad \text{at } y = H \quad (4)$$

where T denotes the fin temperature. x and y are the Cartesian coordinates. L, H and t denote the length, height and thickness of the fin, respectively. h(x,y) is the unknown heat transfer coefficient. k_f is the thermal conductivity of the fin. T₀ and T_∞ respectively denote the fin base temperature and the ambient air temperature.

The unknown heat transfer coefficient in each sub-fin region is assumed to a constant. Thus the finite difference form of (1) in the k-th sub-fin region can be expressed as

$$\frac{T_{i+1,j} - 2T_{i,j} + T_{i-1,j}}{\ell_x^2} + \frac{T_{i,j+1} - 2T_{i,j} + T_{i,j-1}}{\ell_y^2} = \frac{2\bar{h}_k}{k_f t} T_{i,j} \quad (5)$$

for i = 1, 2, ..., N_x, j = 1, 2, ..., N_y, k = 1, 2, ..., N. N_x and N_y are, respectively, the number of nodes in the x- and y-directions. ℓ_x and ℓ_y are defined as ℓ_x = L/(N_x - 1) and ℓ_y = L/(N_y - 1). N is the number of sub-fin region.

The finite difference form of the boundary conditions (2)-(4) can be written as

$$T_{2,j} = T_{0,j} \text{ and } T_{N_x-1,j} = T_{N_x+1,j} \text{ for } j = 1, 2, \dots, N_y \quad (6)$$

and

$$T_{i,1} = T_0 \text{ and } T_{i,N_y-1} = T_{i,N_y+1} \text{ for } i = 1, 2, \dots, N_x \quad (7)$$

The difference equations for the nodes at the interface between two neighboring sub-fin regions and the intersection of four neighboring sub-fin regions are similar to those shown in [12]. In order to avoid repetition, they will not be shown in this manuscript.

Rearrangement of (5) in conjunction with their corresponding difference equations can produce the following matrix equation as

$$[K][T] = [F] \quad (8)$$

where [K] is the global conduction matrix. [T] is the matrix representing the nodal temperatures. [F] is the force matrix. The fin temperatures at the selected measurement locations can be obtained from (8) using the Gauss elimination algorithm.

In order to estimate the unknown heat transfer coefficient \bar{h}_j in the j-th sub-fin region, additional information of the measured fin temperatures at N measurement locations can be required. The more the number of the analysis sub-fin region are, the more accurate the estimate of the unknown heat transfer coefficient may be. However, it might be difficult to measure the temperature distribution on the middle fin of the present problem using the infrared thermography. Excessive thermocouples in the fin may also significantly interrupt the

flow and heat transfer behaviors within the fins. Thus, the thermocouple may be applied to measure the fin temperatures at the selected measurement locations. The heat transfer rate dissipated from the j -th sub-fin region q_j can be written as

$$q_j = 2\bar{h}_j \int_{A_j} (T - T_\infty) dA \quad \text{for } j = 1, 2, \dots, N \quad (9)$$

The average heat transfer coefficient on the fin \bar{h} can be defined as [12]

$$\bar{h} = \frac{\int_{A_f} (T - T_\infty) h(x, y) dA}{\int_{A_f} (T - T_\infty) dA} \quad (10)$$

and

$$\bar{h} = \int_{A_f} \bar{h} dA / A_f \quad (11)$$

Due to limitations of the number of thermocouples, (10) and (11) may not be suitable for the present study. Thus, the average heat transfer coefficient may be approximated as [12]

$$\bar{h} \approx \frac{\sum_{j=1}^N \bar{h}_j A_j}{A_f} \quad (12)$$

and

$$\bar{h} \approx \frac{\sum_{j=1}^{N_{tf}} h_j}{N_{tf}} \quad (13)$$

where h_j denotes the heat transfer coefficient at the j -th grid point. N_{tf} represents the total number of grid points on the lateral surface. A_f and A_j are represented, respectively, lateral surface area of the fin and area of the j -th sub-fin region. The average heat transfer coefficient \bar{h} on the fin is obtained from (12) for the inverse method and from (13) for the commercial software FLUENT.

The actual total heat transfer rate dissipated from the fin to the ambient Q can be expressed as

$$Q = \sum_{j=1}^N q_j \quad (14)$$

The heat transfer coefficient based on the fin base temperature can be defined as

$$\bar{h}^{iso} = \frac{Q}{2A_f(T_o - T_\infty)} \quad (15)$$

The least-squares minimization technique can be applied to minimize the sum of the squares of the deviations between the calculated and measured fin temperatures at the selected measurement locations. The error in the estimates $E(\bar{h}_1, \bar{h}_2, \dots, \bar{h}_N)$ is minimized and is defined as

$$E(\bar{h}_1, \bar{h}_2, \dots, \bar{h}_N) = \sum_{j=1}^N \left[T_{j,inv}^{cal} - T_j^{mea} \right]^2 \quad (16)$$

where T_j^{mea} and $T_{j,inv}^{cal}$ are, respectively, the experimental and calculated fin temperatures at the j -th measurement location. $T_{j,inv}^{cal}$ is determined from (8).

The estimated value of \bar{h} for $j = 1, 2, \dots, N$ can be determined if the value of $E(\bar{h}_1, \bar{h}_2, \dots, \bar{h}_N)$ is minimum. The details of estimating the unknown value \bar{h}_j can be found in [11]. In order to avoid repetition, they are not shown in this manuscript. The computational procedure of this study is repeated until the value of $|(T_j^{mea} - T_{j,inv}^{cal}) / T_j^{mea}|$ for $j = 1, 2, \dots, N$ is less than 10^{-5} . Once the value of \bar{h}_j for $j = 1, 2, \dots, N$ is determined, \bar{h} and \bar{h}^{iso} can be obtained from (12) and (15).

III. THREE-DIMENSIONAL NUMERICAL ANALYSIS

A half section of a fin is selected for the computation of the commercial software. Under the assumptions of the steady-state and constant thermal properties, the three-dimensional heat conduction equation for the thin fin can be expressed as

$$\frac{\partial^2 T}{\partial x^2} + \frac{\partial^2 T}{\partial y^2} + \frac{\partial^2 T}{\partial z^2} = 0, \quad 0 < x < L, 0 < y < H, 0 < z < t/2 \quad (17)$$

The boundary conditions at $z = 0$ and $z = t/2$ can be expressed as

$$-k_f \frac{\partial T}{\partial z} = h(T - T_\infty) \quad \text{at } z = t/2 \quad (18)$$

and

$$\frac{\partial T}{\partial z} = 0 \quad \text{at } z = 0 \quad (19)$$

where x , y and z are the Cartesian coordinates.

Many researchers used various numerical methods to investigate the heat transfer characteristics of plate-fin and tube heat exchangers. However, little information is available in the open literature to investigate the effect of the grid points on the numerical results. Therefore, the present study applies computational fluid dynamics commercial software FLUENT [10] with the k - ϵ model to determine the heat transfer and fluid flow characteristics within the fins of a plate-fin heat sink on heated horizontal plate for various values of the fin spacing S .

Understanding the details of the local heat transfer and fluid flow distributions within the fins can be very important in the design of the heat sink. At the same time, in order to validate the accuracy of the present results further, the computational fluid dynamics commercial software FLUENT [10] in conjunction with the experimental temperature data is also applied to determine the heat transfer coefficient and fin temperature. The ambient air with constant properties can be assumed to be incompressible. The flow within the fins of the heat sink may be assumed to be three-dimensional, symmetric, turbulent, steady and no viscous dissipation. Due to the fin base

temperature higher than the ambient temperature, the buoyancy effect is considered. The laminar flow and the $k-\varepsilon$ turbulence model are applied to simulate the flow within the fins. It is found that the $k-\varepsilon$ model can be the best one even if the Rayleigh number is smaller than 2.5×10^3 .

Thus, the flow within the fins is modeled by the $k-\varepsilon$ model. The continuity, momentum and energy equations within the fins are expressed in tensor form as

$$\frac{\partial u_i}{\partial x_i} = 0 \quad (20)$$

$$\rho u_j \frac{\partial u_i}{\partial x_j} = -\frac{\partial p}{\partial x_i} + \mu \frac{\partial}{\partial x_j} \left(\frac{\partial u_i}{\partial x_j} + \frac{\partial u_j}{\partial x_i} - \frac{2}{3} \delta_{ij} \frac{\partial u_k}{\partial x_k} \right) - \rho \overline{\frac{\partial u_i u_j}{\partial x_j}} \quad (21)$$

and

$$\rho u_j \frac{\partial T_a}{\partial x_j} = k_a \frac{\partial^2 T_a}{\partial x_j^2} - \rho c_p \overline{\frac{\partial u_j T_a}{\partial x_j}} \quad (22)$$

where x_i , $i = 1, 2, 3$, are respectively x , y and z . u_i , p , T_a and g_j are a component of the velocity, pressure, air temperature and gravitational acceleration in the x_j direction, respectively. β is the volumetric thermal expansion coefficient. δ_{ij} is the Kronecker delta. ρ , ν , c_p and k_a are respectively the density, laminar kinematic viscosity, specific heat and thermal conductivity of the air. They are all assumed to be constant. The Reynolds stress tensor and turbulent heat fluxes in conjunction with the Boussinesq approximation are given as

$$-\rho u_i u_j = 2\mu_t S_{ij} - \frac{2}{3}(\rho k + \mu_t \frac{\partial u_i}{\partial x_i})\delta_{ij} \quad (23)$$

and

$$-\rho c_p u_i T_a = k_a \frac{\partial T_a}{\partial x_j} \quad (24)$$

where the mean strain rate tensor S_{ij} is defined as $S_{ij} = \frac{1}{2}(\frac{\partial u_i}{\partial x_j} + \frac{\partial u_j}{\partial x_i})$. Pr_t is the turbulent Prandtl number. The turbulent viscosity μ_t is defined as $\mu_t = \rho c_\mu k^2 / \varepsilon$.

The k and ε equations of this model with the buoyancy effect can be expressed as:

$$\rho u_j \frac{\partial k}{\partial x_j} = \frac{\partial}{\partial x_j} \left[\left(\mu + \frac{\mu_t}{\sigma_k} \right) \frac{\partial k}{\partial x_j} \right] + G_k + G_b - \rho \varepsilon \quad (25)$$

and

$$\rho u_j \frac{\partial \varepsilon}{\partial x_j} = \frac{\partial}{\partial x_j} \left[\left(\mu + \frac{\mu_t}{\sigma_\varepsilon} \right) \frac{\partial \varepsilon}{\partial x_j} \right] + c_{1\varepsilon} \frac{\varepsilon}{k} G_k - c_{2\varepsilon} \rho \frac{\varepsilon^2}{k} \quad (26)$$

where σ_k and σ_ε are turbulent Prandtl numbers for k and ε , respectively. G_k is the production of turbulent kinetic energy

due to the velocity gradient. G_b is the production of turbulent kinetic energy due to buoyancy. They are defined as:

$$G_k = \mu_t \left(\frac{\partial u_i}{\partial x_j} + \frac{\partial u_j}{\partial x_i} \right) \frac{\partial u_i}{\partial x_j} \quad (27)$$

and

$$G_b = \beta g_j \frac{\mu_t}{Pr_t} \frac{\partial T_a}{\partial x_j} \quad (28)$$

where Pr_t is the turbulent Prandtl number for energy. The values of Pr_t , c_μ , $c_{1\varepsilon}$, $c_{2\varepsilon}$, σ_k and σ_ε are given as $Pr_t = 0.85$, $c_\mu = 0.09$, $c_{1\varepsilon} = 1.44$, $c_{2\varepsilon} = 1.92$, $\sigma_k = 1.0$ and $\sigma_\varepsilon = 1.3$. The terms $c_{1\varepsilon}(\varepsilon/k)G_k$ and $c_{2\varepsilon}\rho(\varepsilon^2/k)$ represented, respectively, the shear generation and viscous dissipation of ε .

The matching condition of the temperature and heat flux at the fin-fluid interface can be written as:

$$T = T_a \quad \text{and} \quad k_f \frac{\partial T}{\partial z} = k_a \frac{\partial T_a}{\partial z} \quad (29)$$

At the solid surface, no-slip conditions are specified. The fin base temperature T_0 is constant. The fin temperature at selected measurement locations, T_∞ and T_0 are obtained from the present experiment. The boundary condition of top wall is constant temperature T_∞ . Other walls are adiabatic.

IV. EXPERIMENTAL APPARATUS

The present experiment is conducted in a closed rectangular enclosure. The length, width and height of the rectangular enclosure are $L_e = 0.39$ m, $W_e = 0.16$ m, $H_e = 0.39$ m, respectively. The test fin with 0.1 m in length and 0.001 m in thickness is made of stainless material AISI 304. Two different values of fin height, $H = 0.04$ m and $H = 0.06$ m, are used. The ambient air temperature and the fin temperature are measured using the T-type thermocouple. The diameter of the T-type thermocouple is about 0.13 mm. The limit of its error is $\pm 0.4\%$ for $0^\circ\text{C} \leq T \leq 350^\circ\text{C}$. The schematic diagram of three parallel rectangular fins mounted on the top surface of a heated horizontal plate is shown in Fig. 2. In order to heat three parallel fins, a square heater with 0.08 m in length is fixed on the bottom of this plate using the adhesive tapes (Nitto Denko Co., Ltd). The test fins and horizontal plate enclosed with an insulation material are heated to about 7600 seconds using 40W heater. Four thermocouples placed in a gap between the fins and the horizontal plate and are fixed to $(L/5, 0)$, $(2L/5, 0)$, $(3L/5, 0)$ and $(4L/5, 0)$. The average of the four measured temperatures is taken as the fin base temperature T_0 . Contact thermal resistance between the fin and the horizontal plate is assumed to be negligible. The ambient air temperature T_∞ is measured at 0.3 m over the fin.

TABLE I
 COMPARISON OF T_j , \bar{h} AND \bar{h}^{iso} FOR $S = 0.02$ m AND VARIOUS VALUES OF H

	H = 0.04 m		H = 0.06 m	
	$T_0 = 348.32$ K,		$T_0 = 347.32$ K	
	$T_\infty = 311.92$ K		$T_\infty = 310.79$ K	
	T_{mea}	T_{num}	T_{mea}	T_{num}
T_1	343.13	341.38	334.26	333.92
T_2	343.14	341.39	334.16	333.92
T_3	335.41	336.17	327.57	327.61
T_4	335.43	336.19	327.34	327.61
T_5	330.72	332.56	324.78	323.90
T_6	330.88	332.58	324.67	323.90
T_7	329.21	330.40	323.13	321.90
T_8	329.27	330.41	323.34	321.90
\bar{h}	Inverse	9.27	8.11	
(W/m ² -K)	FLUENT	9.37	7.84	
\bar{h}^{iso}	Inverse	5.83	5.11	
(W/m ² -K)	FLUENT	6.04	4.41	
	Ref. [13]	5.21	5.02	
Ra_s		2.21×10^3	1.94×10^3	
N_t		412587	1464384	

V. RESULTS AND DISCUSSION

All physical properties are evaluated at the average temperature of the fin base and ambient air temperatures. All computations are performed with $0.005 \leq t/S \leq 0.2$, $k_f = 14.9$ W/m-K. $N_x = 21$ and $N_y = 17$ are performed for the inverse method and commercial software FLUENT. The commercial software FLUENT [10] is applied to determine the heat transfer characteristics within the fins of the plate-fin heat sink. An unstructured grid system containing a non-uniform distribution of the grid points is used to determine all of the numerical results. High density grid points between the fins and the coarse grid points in the remainder of the closed enclosure are used. The initial guess of the unknown heat transfer coefficients \bar{h}_j is taken as unity for the inverse method. The rectangular fin is divided into eight regions, i.e., $N = 8$. The eight thermocouples are fixed at the selected positions on the fin, as shown in Fig. 1. T_j^{num} denotes the fin temperature obtained using the commercial software FLUENT [10] at the j -th measurement location.

Various heat transfer correlations have been proposed for the present problem for the natural convection heat transfer from the plate-fin heat sinks. Among these heat transfer correlations, correlations from [13] may be selected to be compared with the results obtained.

An empirical correlation can be obtained from [13] as follows

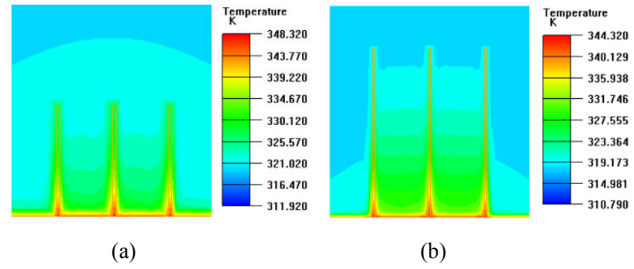
$$Nu = \left[\left(\frac{Ra_s}{1500} \right)^{-2} + (0.081 Ra_s)^{0.39} \right]^{-0.5} \quad (30)$$

where $200 \leq Ra_s \leq 6 \times 10^5$ and $0.016 \leq S/L \leq 0.20$. The Rayleigh number Ra_s and the Nusselt number Nu are defined as follows:

$$Ra_s = \frac{g\beta(T_0 - T_\infty)S^3}{\alpha\nu} \quad (31)$$

and

$$Nu = \frac{\bar{h}^{iso} S}{k_{air}} \quad (32)$$


 Fig. 3 Temperature distribution between plate-fins for $S = 0.02$ m
 (a) $H = 0.04$ m, (b) $H = 0.06$ m

Comparison of T_j , \bar{h} and \bar{h}^{iso} is shown in Table I for two different values of H and $S = 0.02$ m. It is found that the values of \bar{h}^{iso} obtained from the inverse method slightly deviate from those from (30). In order to determine a more accurate numerical result, the appropriate grid points may be selected such that the numerical results of \bar{h} and \bar{h}^{iso} are as close as possible to those obtained from the inverse method. In addition, the difference of the experimental data and numerical fin temperature is also small at the selected measurement locations. Table I shows that the numerical results of \bar{h} and \bar{h}^{iso} are in good agreement with those obtained from the inverse method. The calculated temperature of the fin at selected measurement locations also agrees with the experimental data. This implies that the present results have good accuracy and good reliability. The obtained results of \bar{h} and \bar{h}^{iso} decrease with increasing fin height. An interesting finding is that the total number of grid points N_t increases with the fin height. The value of N_t varies with the fin height

Fig. 3 shows the temperature distribution of the air between the fins for $z = 0.5$ mm, $S = 0.02$ m and $H = 0.04$ m and 0.06 m. The fins have a higher temperature and the temperature gradient close to the fin base, as shown in Table I. The temperature variation in the vicinity of the fin base seems to be enormous.

VI. CONCLUSION

The present study proposes the inverse method and the computational fluid dynamics commercial software FLUENT in conjunction with the experimental temperature data to determine the heat transfer characteristics within the fins of plate-fin heat sink. The results show that the present numerical results of \bar{h} and \bar{h}^{iso} using the k - ϵ model are in good agreement with the present inverse results. The present inverse and numerical results of \bar{h}^{iso} also agree with those obtained from [13]. This implies that the present results are reliable. This implies that the application of the k - ϵ model to solve the present problem is appropriate. The total number of grid points may vary with the fin height in order to obtain more accurate results. The commercial software FLUENT in conjunction with inverse results or experimental data can be applied to obtain a more accurate heat transfer characteristics of plate-fin heat sink with an appropriate flow model and grid points. This study is useful in electronics cooling applications.

ACKNOWLEDGMENT

The authors gratefully acknowledge the financial support provided by the National Science Council of the Republic of China under Grant No. NSC 102-2221-E-006-177-MY3. We would also like to thank Professor Chin-Hsiang Cheng at National Cheng Kung University to give us the commercial software FLUENT.

REFERENCES

- [1] W. Elenbass, "Heat dissipation of parallel plates by free convection," *Physical*, Vol. 9, pp. 2-28, 1942.
- [2] E. M. Sparrow, P. A. Bahrami, "Experiments on natural convection between heated vertical plates with either open or closed edges," *ASME J. Heat Transfer*, vol. 102, pp. 221-227, 1980.
- [3] J. R. Bodoia, J. F. Osterle, "The development of free convection between heat vertical plates," *ASME J. Heat Transfer*, vol. 84, pp. 40-44, 1962.
- [4] A. de Lieto Vollaro, S. Grignaffi, F. Gugliemetti, "Optimum design of vertical rectangular fin arrays," *Int. J. Therm. Sci.*, vol. 38, pp. 525-529, 1999.
- [5] S. Baskaya, M. Sivrioglu, M. Ozek, "Parametric study of natural convection heat transfer from horizontal rectangular fin arrays," *Int. J. Therm. Sci.*, vol. 39, pp. 797-805, 2000.
- [6] F. Harahap, D. Setio, "Correlations for heat dissipation and natural convection heat transfer from horizontally-based, vertically-finneed arrays," *Appl. Energy*, vol. 69, pp. 29-38, 2001.
- [7] S. A. Nada, "Natural convection heat transfer in horizontal and vertical closed narrow enclosure with heated rectangular finned base plate," *Int. J. Heat Mass transfer*, vol. 50, pp. 667-679, 2007.
- [8] H. G. Yalcin, S. Baskaya, M. Sivrioglu, "Numerical analysis of natural convection heat transfer from rectangular shrouded fin arrays on a horizontal surface," *Int. Comm. Heat Mass Transfer*, vol. 45, pp. 4957-4966, 2002.
- [9] I. Tari, M. Mehrtash, "Natural convection heat transfer from inclined plate-fin heat sinks," *Int. J. Heat Mass transfer*, vol. 56, pp. 574-593, 2013.
- [10] FLUENT Dynamics Software, FLUENT, Lehanon, NH, 2010.
- [11] H.T. Chen, L.S. Liu, S.K. Lee, "Estimation of heat-transfer characteristics from fins mounted on a horizontal plate in natural convection," *CMES: Computer Modeling in Engineering & Sciences* 65, 155-178, 2010.
- [12] H.T. Chen, S.T. Lai, L.Y. Haung, "Investigation of heat-transfer characteristics in plate-fin heat sink," *Appl. Thermal Eng.* 50, 352-360, 2013.
- [13] G. D. Raithby, K. G. T. Hollands, "Natural Convection," *Handbook of Heat Transfer Fundamentals*, 2nd ed., W. M. Rohsenow, J. P. Hartnett and E. N. Ganic, eds, McGraw-Hill, New York, 1985.